Frequency Analysis of Semiconductor Devices using Full-Band Cellular Monte Carlo Simulations.

J. Branlard*, S. Aboud+*, P. Osuch*, S. Goodnick†, and M. Saraniti*+

Abstract— **The goal of this work is to use a particle-based simulation tool to perform a comparative study of two techniques used to calculate the small signal response of semiconductor devices. Several GaAs and Si devices have been modeled, simulated in the frequency domain to derive their frequency dependent complex output impedance. Conclusions are drawn regarding the applicability and advantages of both approaches.**

Keywords— **particle-based simulation, full-band, Fourier Decomposition, small-signal analysis, GaAs MESFETs, SOI MOSFETs.**

I. Full-band, particle-based CMC

Particle-based methods are based on the semi-classical description of charge transport through the stochastic solution of the Boltzmann Transport Equation (BTE) [1], coupled with a self-consistent solution of Poisson's Equation (PE), used to account for the spacial variation of the quasi-static electric field. The PE is solved using a multi-grid algorithm [2], and the field is updated often enough so as to resolve plasma oscillations [3]. A full-band representation [3] of the electron dispersion relation, calculated using the empirical pseudopotential method [4] is used. Local, nonlocal and spin-orbit interactions are included in the band structure calculation. The full phonon spectra of the semiconductor materials discussed in this work are calculated over the first Brillouin Zone (BZ) with a valence shell model [3]. Scattering with deformation potential optical and acoustic phonons and polar optical phonons is accounted for. The screening model used for impurity scattering is the Ridley model as discussed in [3]. The carrier dynamics is simulated with the Cellular Monte Carlo approach [5], where all of the possible final momentum states for each initial electronic state and for all possible scattering mechanisms are pre-calculated and stored in large look-up tables. This approach reduces the final state selection process during run-time to the generation of a single random number, and is up to 50 times faster than the Ensemble Monte Carlo approach for bulk simulations [6].

*Electrical and Computer Engineering Department, Illinois Institute of Technology, Chicago, IL 60616, USA Corresponding author: Julien Branlard, phone: (312) 567 3413, fax: (312) 567 5733, email: julien@neumann.ece.iit.edu

+Department of Molecular Biophysics, Rush University, Chicago, IL, USA

†Electrical Engineering Department, Arizona State University, Tempe, AZ, USA

II. Frequency analysis, two approaches

A common approach to extract the small-signal parameters of a device is to apply to one of its electrodes a small perturbation about a steady-state condition, while keeping all other parameters constant. In the case of a sinusoidal perturbation applied to the drain of a FET, the source potential is grounded, a constant bias V_{GS} is applied to the gate and $\tilde{v}_{DS}(t) = V_0 sin(\omega_0 t)$ represents the variations of the drain voltage. To ensure small-signal conditions, the amplitude V_0 of the sinusoidal excitation is one or two orders of magnitude smaller than the applied DC voltages, and $V_{DS} \pm V_0$ remains in the saturation region of the current-voltage characteristic of the transistor. The sinusoid is simulated for one full period T, setting the input frequency of the voltage perturbation $\omega_0 = 2\pi/T$. The frequency analysis is performed with Fourier transforms, given for the drain voltage variations by,

$$\begin{aligned} \hat{v}_{ds}(\omega) &= \int_{-\infty}^{+\infty} (\tilde{v}_{ds}(t)) e^{-j\omega t} dt, \\ &= V_0 \frac{\omega_0}{\omega^2 - \omega_0^2} \Big(e^{-j2\pi \frac{\omega}{\omega_0}} - 1 \Big), \end{aligned} \tag{1}$$

where the $(\hat{x})$ symbol denotes the Fourier transformed variable. At $\omega = \omega_0$, the Eq. 1 simplifies to $\hat{v}_{ds}(\omega) = V_0 \pi / j\omega_0$ and equals zero for harmonics $\omega_k = k\omega_0$ with $k \neq 1$, $\hat{v}_{ds}(\omega_k) = 0$. In a similar manner, the transient drain current response $\tilde{i}_d(t) = i_d(t) - I_{ss}$ is also analyzed in the frequency

domain. Its Fourier transform $\hat{i}_d(\omega)$ is given by,

$$\begin{aligned}\hat{i}_d(\omega) &= \int_0^T \tilde{i}_d(t)e^{-j\omega t}dt, \\ &= DT\sum_{n=0}^{N-1}\tilde{i}(nDT)e^{-j\omega nDT},\end{aligned} \tag{2}$$

where I_{ss} is the initial and the final steady-state, the simulation time T is sampled into N steps of duration DT, at the end of which the drain current variation is sampled. The frequency-dependent admittance $\hat{Y}_{22}(\omega)$ is then obtained as the ratio of the Fourier-transformed drain current variations, and the Fourier-transformed drain voltage variations. Due to the monochromatic nature of the perturbation, the energy of the signal is mainly centered around the input frequency ω_0. Consequently, an optimal noise-to-signal ratio is obtained for $\omega = \omega_0$. At $\omega = \omega_0$, the corresponding complex impedance Z_{out} can be expressed as,

$$Z_{out}(\omega_0) = (\hat{Y}(\omega_0))^{-1} = R(\omega_0) + jX(\omega_0), \tag{3}$$

where $R(\omega_0)$ and $X(\omega_0)$ are the resistance and the reactance, respectively.

Values of the output impedance at different frequencies can then be obtained by applying perturbations at the drain electrode, at different frequencies and computing the resulting complex impedance. The major advantages of this method are its simplicity, robustness and flexibility because there are no limitations in terms of frequency resolution. Sparse measurements can be achieved in the regions of low variations, finer ones where the impedance undergoes rapid changes. On the other hand, the analysis based on monochromatic perturbation becomes computationally expensive if a wide frequency survey of the output impedance behavior is needed, as the number of required simulations is as large as the spectrum is. To overcome this issue, the Fourier decomposition [7], [8], [9] offers an alternative frequency analysis approach. A step voltage of amplitude ΔV_0 is applied to the drain electrode, during a time T long enough to allow for the drain output current response to recover steady-state. The drain current is thus taken from an initial steady-state I_{ss_1} to a final steady-state I_{ss_2} over the time period T. The Fourier transform of both the voltage and the current variations is taken,

$$\hat{v}_{ds}(\omega) = \frac{\Delta V_0}{j\omega}. \tag{4}$$

and,

$$\hat{i}_d(\omega) = \int_0^T \tilde{i}_d(t)e^{-j\omega t} + \int_T^{+\infty}\Delta I e^{-j\omega t}, \tag{5}$$

assuming that after a time T, the current response reaches a final steady-state I_{ss_2}, and the current variation after $t = T$ is $\Delta I = I_{ss_2} - I_{ss_1}$. In the discrete time case, Eq. 5 becomes,

$$\hat{i}_d(\omega) = DT\sum_{n=0}^{N-1}\tilde{i}_d(nDT)e^{-j2\pi\frac{kn}{N}} + \Delta I\frac{e^{-j\omega T}}{j\omega}, \tag{6}$$

where the simulation time $T = NDT$ and the discrete frequencies ω_k are given by $\omega_k = 2\pi k/T$ for $k = 0, 1, ..., N/2$. The complex frequency-dependent impedance can be derived in the same manner as for the monochromatic excitation. The frequency resolution of the method is determined by the total simulation time T, whereas the upper limit of the analyzed spectrum f_{max} is set by the sampling time-step DT as $\Delta\omega = 1/T$ and $f_{max} = 1/2DT$. The major advantage of this approach is its computational efficiency, in fact, the entire spectrum can be spanned with a single simulation. Whereas a monochromatic sinusoidal function only carries one single frequency, the step voltage conveys the whole frequency spectrum. It is therefore appropriate for a broadband frequency analysis of semiconductor devices. However, obtaining a fine frequency resolution can be an issue as it requires an inversely large simulation time. For finer analysis of a particular frequency interval, the sinusoidal excitation approach is more appropriate.

III. Results

These two techniques have been tested on various semiconductor devices. Figure 1 shows a plot of the resistance and the reactance versus frequency for a Gallium Arsenide MEtal Semiconductor Field Effect Transistor, (GaAs MESFET) with a gate length $L_G = 100$ nm and a donor concentration $N_D = 10^{18}$ cm^{-3}. Each couple $\{R(\omega), X(\omega)\}$ represents one simulation obtained with the monochromatic excitation approach.

The frequency f_m at which the reactance reaches its maximum negative value is related to the characteristic relaxation time τ measuring the minimum switching time of the device,

$$\tau = 2\pi f_m. \tag{7}$$

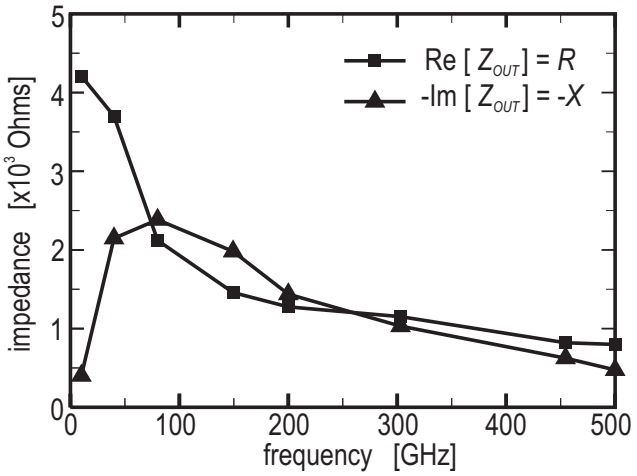

Fig. 1. Variations of the Complex Output Impedance with Frequency, for a 100 nm long GaAs MESFET.

The output voltage gain falls rapidly for frequencies higher than f_m and for this reason, it is often referred to as the cut-off frequency. For the simulated GaAs MESFET device, a cut-off frequency $f_m = 80$ GHz is found, and falls in the expected frequency range for such devices [10].

To illustrate the implementation of the Fourier decomposition approach, a Silicon On Insulator Metal Oxide Semiconductor FET (SOI-MOSFET) inspired by a recent INTEL publication [11] has been simulated. Its gate length is $L_G = 70$ nm, the donor and acceptor concentrations are $N_D = 10^{20}$ and $N_A = 10^{14}$ cm^{-3}, respectively, and the insulator thickness is 1.5 nm, as illustrated in Fig. 2. DC characterization of the device has been achieved and full IV curves have been simulated.

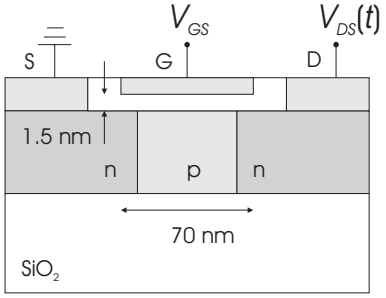

Fig. 2. Schematic layout of a SOI-MOSFET, with a 70 nm wide gate length and a 1.5 nm thick oxide layer.

To perform the small-signal analysis of the device, a step voltage $\Delta V = 0.2$ V has been applied to the drain electrode, while the initial biases $V_{DS} = 0.5V$ and $V_{GS} = -1.0$ V have been simulated for 10 ps to place the device in steady-state. The drain step-voltage is maintained for 50 ps which corresponds to a frequency resolution $\Delta f = 20$ GHz. Figure 3 shows the real and the imaginary part of the output impedance versus frequency.

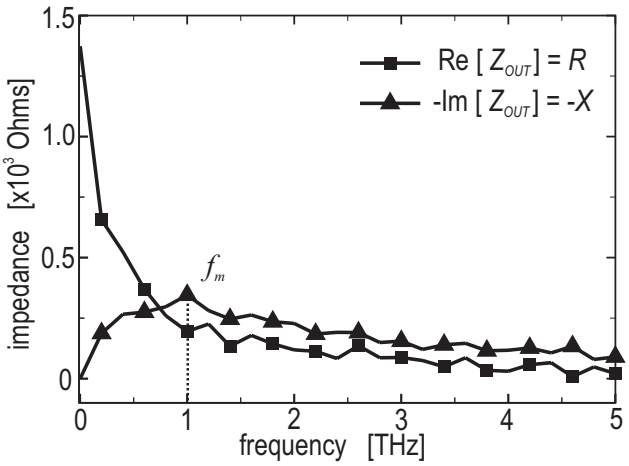

Fig. 3. Variations of the Complex Output Impedance with Frequency, for a 70 nm long SOI MOSFET.

Unlike the sinusoidal excitation case, this curve is obtained by only one simulation. A cut-off frequency of approximately 1 THz is found, which agrees with its announced terahertz application range.

When applied to the same device, the Fourier decomposition and the sinusoidal excitation yield similar results, as illustrated on Fig. 4. The simulated device is a GaAs MESFET with a gate length $L_G = 98$ nm and a donor concentration $N_D = 5 \times 10^{17}$ cm^{-3}. The applied steady-state biases are $V_{DS} = 1$ V and $V_{GS} = -1.0$ V. To account for Fermi level pinning effects, a positive bias of +0.6 V has been applied at the top of the device, between the source and the gate, and between the gate and the drain. A drain step voltage of amplitude 0.2 V has been simulated for 50 ps to ensure a frequency resolution of 20 GHz. On Fig. 4, the solid line shows the frequency-dependent output resistance and reactance obtained with Fourier decomposition approach, while those obtained with sinusoidal excitations are represented by the discrete points.

Although a good agreement is observed, more work needs to be done to fully compare the two approaches. A noise analysis could determine whether one is more stable or less noisy than the other. In the case of the Fourier decomposition, the amplitude of the applied step voltage should

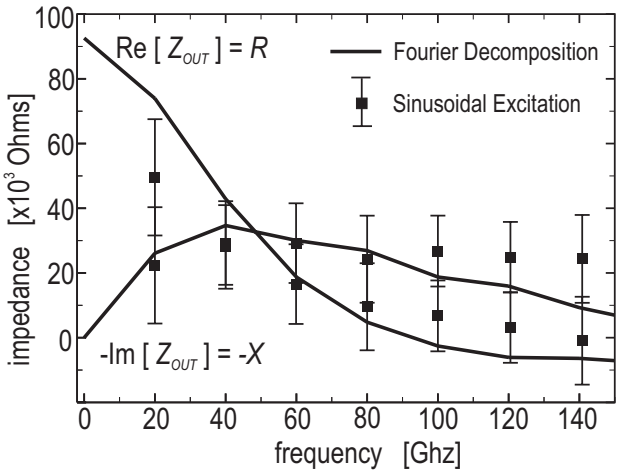

Fig. 4. Frequency-dependent output impedance of a 98 nm wide GaAs MESFET, obtained with the Fourier decomposition approach, (solid line) and with 10 monochromatic sinusoidal excitations (discrete points).

stay in the small-signal range (i.e. several hundred millivolts) [9]. However, for devices showing a strong drain current saturation, a small amplitude drain step-voltage does not yield appreciable drain current variation, and makes the extraction of significant transients challenging. On the other hand, the use of a larger step-voltage might results in apparition of harmonics in the current response. Although large step voltages have been applied, such harmonics have not been observed. Further investigation is required to understand why and to see the impact of applying large step-voltage on the device transient characteristics. Although rather noisy for certain devices,the transient output current does not require smoothing in the context of this work. In fact, when shifting to the frequency domain, the Fourier transforms performs a systematic filtering. The discrete Fourier transforms implemented in this work are a 0^{th} order approximation. Higher orders discrete models have been implemented, and investigated. Their benefit allows to reduce aliasing observed at high frequencies. However, the investigated device frequencies are one or two order of magnitude smaller than that where aliasing occurs, and consequently, the use of higher order Fourier transforms is not relevant for the purpose of this work.

IV. Conclusion

Two approaches to perform a small-signal investigation of semiconductor devices have been described and implemented to analyze the frequency-dependent output impedance of several GaAs MESFETs and a SOI-MOSFET. The simulated small-signal parameters show good agreement with published data, and a comparison of the two approaches when applied to a same device shows comparable results. While the main advantage of the Fourier decomposition is that it allows to span the entire frequency spectrum with one simulation, its main restriction comes from the requirement in long simulation times to achieve fine frequency resolution. This is avoided within the monochromatic sinusoidal excitation formalism. More work needs to be to fully compare the stability and applicability of both methods.

References

[1] D.A. McQuarrie, *Statistical Mechanics*, University Science Books, Sausalito, CA, 2000.

[2] M. Saraniti, *Development of efficient numerical techniques for semiconductor device simulations*, Ph.D. thesis, Technische Universität München - Germany, July 1996.

[3] M.V. Fischetti and S.E. Laux, "Monte Carlo analysis of electron transport in small semiconductor devices including band-structure and space-charge effects," *Physical Review B*, vol. 38, no. 14, pp. 9721–9745, Nov. 1988.

[4] Mavin L. Cohen and T. K. Bergstresser, "Band structures and pseudopotential form factors for fourteen semiconductors of the diamond and zinc-blende structures," *Physical Review*, vol. 141, no. 2, pp. 789–796, January 1966.

[5] C. Jacoboni, ," Private Communication, Sept. 2001, International Workshop on Monte Carlo methods. Salzburg, Austria.

[6] M. Saraniti and S.M. Goodnick, "Hybrid full-band Cellular Automaton/Monte Carlo approach for fast simulation of charge transport in semiconductors," *IEEE Transactions on Electron Devices*, vol. 47, no. 10, pp. 1909–1915, October 2000.

[7] R.W. Hockney and J.W. Eastwood, *Computer Simulation Using Particles*, Adam Hilger, Bristol, 1988.

[8] R. A. Warriner, "Computer simulation of gallium arsenide field-effect transistors using Monte-Carlo methods," *IEE Solid State and Electron Devices*, vol. 1, no. 4, pp. 105–110, July 1977.

[9] S.E. Laux, "Techniques for small-signal analysis of semiconductor devices," *IEEE Transactions on Electron Devices*, vol. ED-32, no. 10, pp. 2028–2037, Oct 1985.

[10] F. Schwierz and J.J. Liou, *Modern Microwave Transistors, theory, design and performance*, Wiley InterScience, 2003.

[11] R. Chau, J. Kavalieros, B. Doyle, A. Murthy, N. Paulsen, D. Lionberger, D. Barlage, R. Arghavani, B. Roberds, and M. Doczy, "A 50 nm depleted-substrate cmos transistor (dst)," *IEDM Technical Digest*, 2001.